

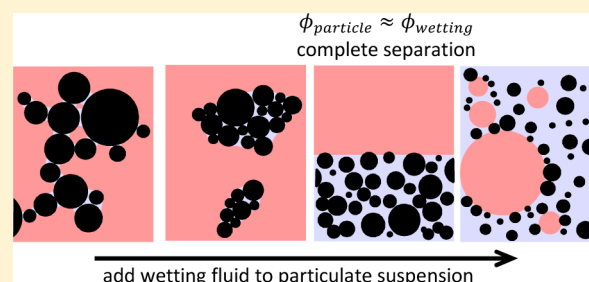
Aggregation and Separation in Ternary Particle/Oil/Water Systems with Fully Wettable Particles

Samantha J. Heidlebaugh, Trystan Domenech, Steven V. Iasella, and Sachin S. Velankar*

Department of Chemical and Petroleum Engineering, University of Pittsburgh, Pittsburgh, Pennsylvania 15261, United States

S Supporting Information

ABSTRACT: We report that a variety of ternary particle/liquid/liquid mixtures heavily aggregate or separate completely if (1) the particles are fully or almost fully wetted by one fluid, and (2) if the wetting fluid volume fraction is comparable to the particle volume fraction. Aggregation and separation do not happen if the particles are partially wetted by both fluids, in which case Pickering emulsions appear at all compositions. Rheological and geometric criteria for aggregation are proposed and compared with a state diagram of a ternary system composed of oil, water, and hydrophilic glass particles. Analogies are drawn to wet granulation and spherical agglomeration, two particle processing operations in which wetting phenomena are important.



1. INTRODUCTION

The past fifteen years have seen enormous research on Pickering emulsions. These systems are composed of two immiscible fluids, often oil and water, with a small quantity of particulate species added. The particles are partially wetted by both fluids (i.e., the contact angle of the liquid–liquid interface at the particle surface is between 0 and 180°) and hence can adsorb at the interface between the two fluids. With suitable mixing, such ternary systems develop specific morphologies that are stabilized by the interfacially adsorbed particles. A variety of morphologies have been observed including particle-covered emulsion drops,^{1–3} particle-bridged drops,^{4–8} or bijels.^{9–12} If one of the fluids is air, particle-stabilized foams,^{13–15} “dry liquids”,^{16,17} or “liquid marbles”^{18–20} can be readily prepared.

All the cases in the previous paragraph correspond to particle/fluid/fluid systems in which the particle volume fraction is typically much lower than the volume fraction of both the fluids. Converse cases where the particle loading is larger than that of one of the fluids have also been examined.^{21–23} These cases correspond to particulate suspensions to which a small quantity of a second immiscible fluid has been added. With suitable mixing, the minority fluid is able to join particles together into a percolating network. If the particles are fully or preferentially wetted by the minority fluid, the microstructure of this network consists of particles bridged by “pendular” capillary bridges.²⁴ If the particles are preferentially wetted by the majority fluid, the microstructure is more complex, consisting of small “capillary clusters” of a few particles held together by drops of the minority fluid.²⁵

Most of the above research on Pickering emulsions and suspensions containing two immiscible fluids is rooted in the idea that interfacial adsorption of particles is extremely strong.¹

However as the contact angle approaches either zero or 180°, the strength of the adsorption reduces sharply and particles can readily detach from interfaces, either due to thermal motion or due to external forces, for example, during mixing. Particle desorption due to viscous forces is especially likely for large particles as explained in greater detail in the Appendix. Of course, one may also have situations where the particles are fully wetted by one of the phases and hence do not adsorb at the interface at all. Such ternary systems in which the particles are nearly or fully wetted by one phase are the subject of this paper. We pose the specific question: what is the structure of the ternary system if the particles are able to desorb from the interface or, equivalently, if the wetting fluid can engulf the particles? One can readily imagine two simple scenarios: if the wetting fluid is the continuous phase, the particles and the drops may be independently suspended in the wetting fluid, in effect, a physical mixture of a suspension and an emulsion (Figure 1a). If the nonwetting fluid is the continuous phase, the particles may be encapsulated within the drops, in effect, an emulsified suspension (Figure 1b). However these are not the only scenarios possible; depending on the location in the ternary composition diagram^{26,27} (Figure 2), the relative size of the particles and drops, and the mixing conditions, pendular aggregates (Figure 1c), double emulsion structures, or more complex morphologies may be possible. Moreover, if the particle loading is high, the viscosity of the particle-containing phase would be high and kinetically-trapped morphologies such as nonspherical drops (Figure 1d) due to internal jamming²⁸ may become likely. This article seeks to clarify some of these

Received: October 14, 2013

Revised: November 26, 2013

Published: December 17, 2013

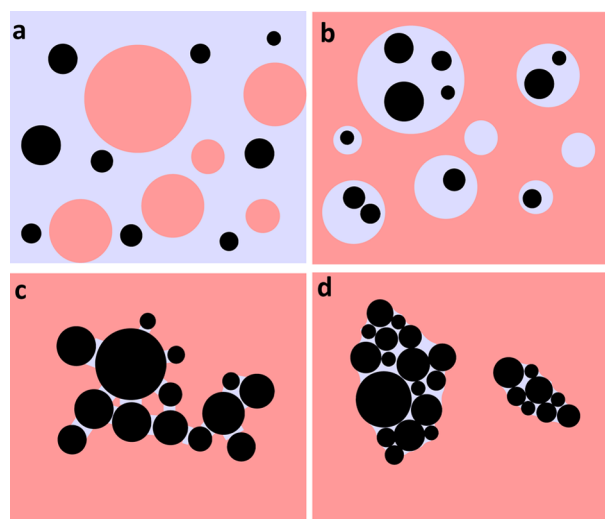


Figure 1. Possible structures of ternary systems where particles (black) are fully wetted by the light blue phase. (a) Wetting phase is continuous. (b) Nonwetting phase is continuous. (c) Pendular network. (d) Capillary aggregates.

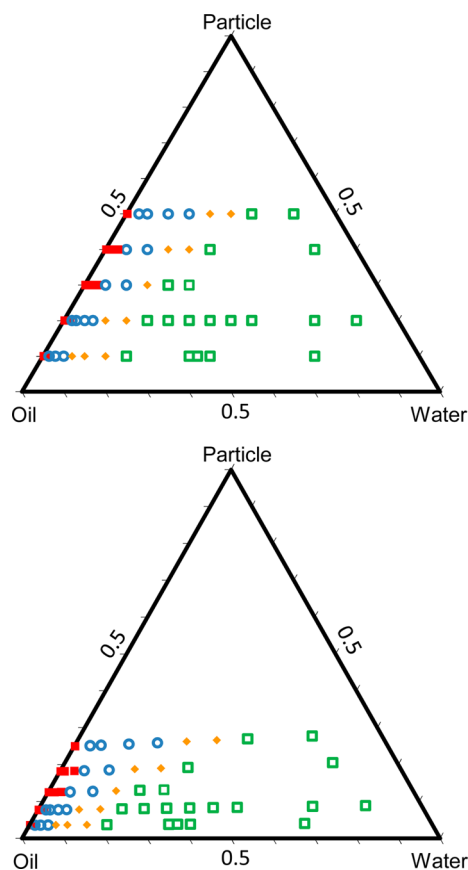


Figure 2. Compositions studied in this paper placed on a ternary composition diagram based on (top) weight and (bottom) volume.

issues experimentally using simple model systems. Specifically, for mixtures of oil, water, and particles that readily desorb off the interface, we map the structure of the ternary mixtures resulting from the applied mixing process. We focus especially on the observation that when the volume fraction of the wetting fluid is comparable to that of the particles, the mixtures aggregate heavily or separate completely into two phases. Such

aggregation and separation appears to be a universal feature in systems with fully wetted particles.

2. EXPERIMENTAL SECTION

Table 1 lists all the materials used in the experiment. Most of the research is conducted with unmodified glass particles of roughly 5 μm

Table 1. Materials Used

material	mean diameter (μm)	density (g/mL)	supplier
glass, unmodified (Figure 3–6, Supporting Information S1a,S2a,S3)	5	2.50	Prizmalite Microspheres
glass unmodified (Supporting Information Figure S1b, S4)	35	2.50	Prizmalite Microspheres
silica, unmodified (Supporting Information Figure S1c, S5)	0.7	2.50	Denka
glass, highly hydrophobic (Supporting Information Figure S2b, S6)	5	2.50	Prizmalite Microspheres
glass, partially hydrophobic (Supporting Information Figure S2c, S8)	5	2.50	Prizmalite Microspheres
silica, unmodified (Supporting Information Figure S1d, S7)	2	2.5	Industrial Powder, Inc.
light mineral oil		0.83	Fischer Scientific
polyethylene oxide MW 35000		1.05	Aldrich
polyisobutylene MW 2400		0.91	Soltex

in diameter. All the figures in the main text of the paper refer to these particles. They are highly hydrophilic and when added to a water-in-oil mixture, most particles are present in the bulk water phase (Supporting Information Figure S2a). Nevertheless, they can still adsorb at the oil/water interface (Figure 3c presented later) but presumably with a small contact angle as measured through the water phase. Figure 2 maps the actual compositions examined in this work in weight and volume fractions (the different symbols used at each composition will be explained later). All the other particles listed in Table 1 were used for only a limited set of experiments, and the corresponding figures are presented as Supporting Information.

Unless otherwise noted, mixtures were prepared as follows. First oil and water (with fluorescein added) were placed in a 6 mL vial at the desired ratio and shaken in a vortex mixer for 45 s. The desired quantity of particles were added to the vial and vortexed again for 45 s. It is important to emphasize that much of the interesting behavior occurs when one of the fluids is dilute (about 3%, which corresponds to less than 0.1 mL for a typical batch size of 3 mL). This can create two complications. First, any mixer whose parts contact the ternary mixture can create significant uncertainty in the actual mixture composition. Even relatively small mixers, for example, Tissumizer or Ultra Turrax T10, can retain volumes on the order of 0.1 mL fluid, and if the internal parts of the mixer are wetted by the minority fluid the composition of the mixture is changed to an unknown extent from its target value. The use of a vortex mixer, and hence the fact that mixing occurs on an entirely closed system, avoids this complication. Second, if the minority fluid wets the walls of the container, it simply smears on the walls, once again causing uncertainty in the composition. Thus, most of this research was conducted with vials whose inner surfaces were hydrophobized with octadecyltrichloromethylsilane. The only exception is Supporting Information Figure S6 where the particles are hydrophobic and the wetting fluid is oil; in these experiments, unmodified vials were used.

Images were taken with a digital camera. Microscopy was conducted on some samples using either an Olympus CKX-41 inverted brightfield microscope or Olympus Fluoview 1000 inverted laser scanning confocal microscope. Rheological measurements of binary particle-in-water suspensions were conducted at 25 $^{\circ}\text{C}$ on an AR2000

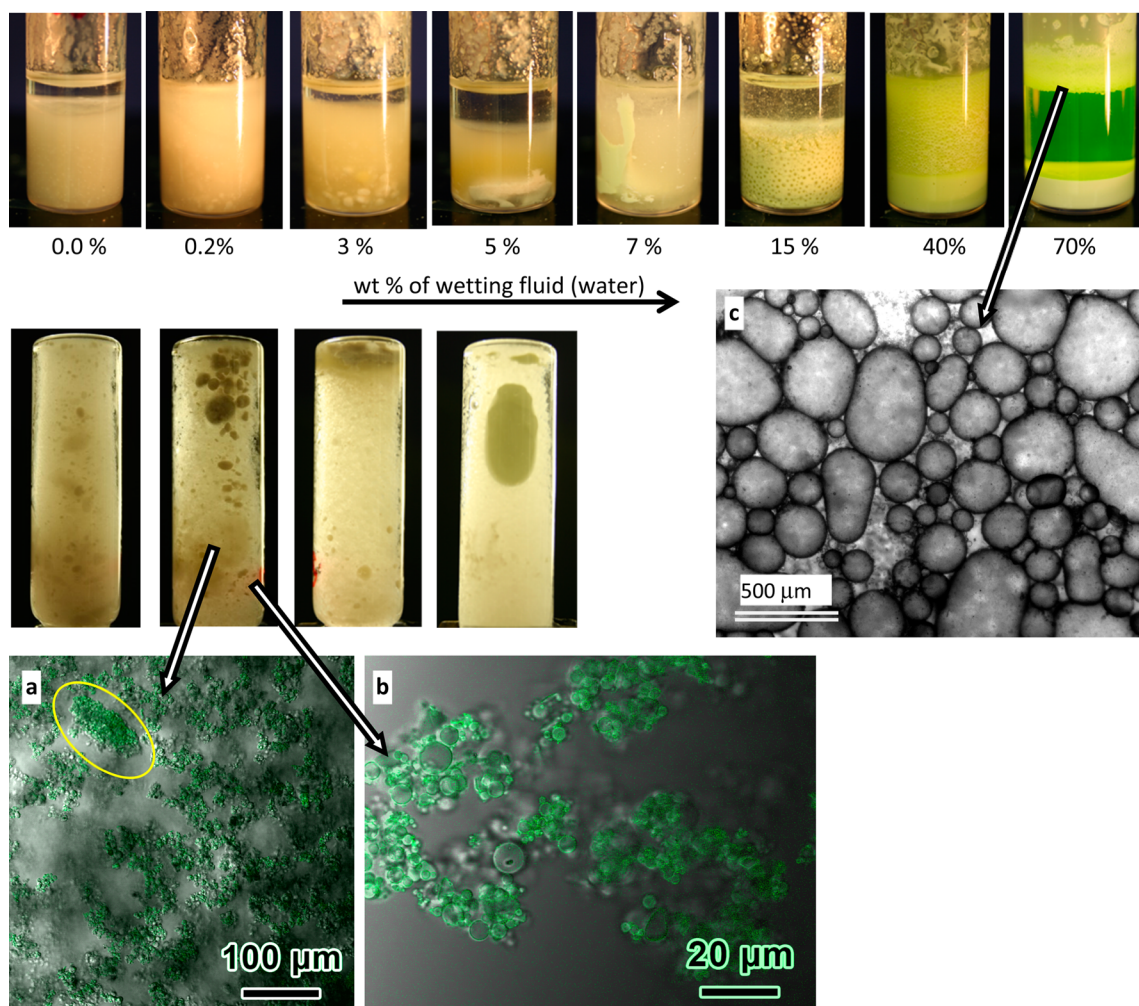


Figure 3. Top row of vials: Structure of mixtures with 20 wt % particles. Middle row shows the same vials as the top row, but laid on the side and photographed from the bottom to show aggregates more clearly. (a,b) Overlay of confocal fluorescence images and DIC images of the vial at 0.2% water and two different magnifications. Fluorescence indicates presence of water. The yellow ellipse in a marks a capillary aggregate of particles. (c) Brightfield image of the oil drops at 70% water.

rheometer using a 25 mm parallel plate geometry. Sandpaper was glued onto the plates to prevent wall slip.

3. RESULTS

3.1. Qualitative Description of Structural Changes with Composition. Figure 3 shows images of mixtures at a fixed particle loading of 20 wt % and successively increasing water loadings, i.e., moving horizontally in the triangular composition diagram of Figure 2a. In the absence of water, the particles sediment to some extent, but the height occupied by the particles is far more than may be expected from their ~ 10 vol % loading. In effect, the particles are able to form a weak attractive network in oil, which is not unreasonable considering their hydrophilicity. At the lowest water content of 0.2%, the entire vial appears cloudy, and sedimentation is eliminated almost completely. This nonsettling behavior indicates the presence of a network structure, and indeed, confocal imaging of this sample (Figure 3a,b) reveals a pendular network but also some small particle aggregates (e.g., circled in yellow in Figure 3a) that include significant amounts of water. However examination of the vials also shows that there are some much larger particle aggregates at the bottom. Tilting the vial to a horizontal position (middle row images in Figure 3) permits a

clearer view of the aggregates, and they appear to be no more than 2 mm in size and irregular in shape. Further increases in water content lead to an increase in the number and size of aggregates until at 5% water a single large aggregate is formed. While a cloudy layer is still evident indicating that some particles remain suspended in oil, for all practical purposes this sample may be regarded as completely phase separated. With a further increase in water content, phase inversion occurs, with millimeter-sized oil drops being dispersed in water. Finally, at all water contents exceeding 20%, the structure of the system consists of a top layer of oil drops floating over a lower aqueous layer within which the particles sediment to the bottom. With increasing water content from 20 to 70%, the oil/particle ratio reduces and so does the size of the oil drops. Optical microscopy (Figure 3c) shows that these oil drops are stabilized by a layer of adsorbed particles, that is, at high water content, the structure is that of a Pickering emulsion except that a large fraction of the particles do not reside at the interface but instead are sedimented to the bottom. The images of Figure 3 were taken within 1 min after vortex-mixing was completed. Upon longer storage under quiescent conditions, gravitational effects became more obvious. For example, the vial with 40% water in Figure 3 also stratified into three layers (floating oil

drops, clear water, sedimented particles), similar to the vial with 70% water. Nevertheless, changes other than sedimentation were not apparent: pendular network structures did not appear to coarsen significantly and Pickering emulsion drops or particle aggregates did not coalesce significantly even after several hours.

Pendular networks and Pickering emulsions are both well-documented in the literature on ternary particle/fluid/fluid systems.^{1,21,22,29} However the formation of compact aggregates and their unbounded growth, which leads to rapid sedimentation and hence macroscopic phase separation, are less familiar and will be examined in detail in this paper. Before proceeding, however, it is useful to test whether the trends of Figure 3 are “universal”, that is, whether they apply to a variety of compositions, fluids, or particle types. Accordingly, the next few paragraphs describe a sequence of experiments testing (1) higher particle loading than Figure 3, (2) larger or smaller hydrophilic particles than Figure 3, (3) hydrophobic particles which are preferentially wetted by oil rather than by water, and (4) substituting the oil and water with two macromolecular, nonaqueous fluids of high viscosity. In all these ternary systems, we show that as the wetting fluid fraction increases, the changes in structure follow the same trends as Figure 3. Finally, we will present a counter-example in which the particles are partially wetted by both phases rather than being nearly fully wetted by one phase. In that case, the structural evolution is sharply different from Figure 3 and specifically, large aggregates do not appear. This unequivocally establishes that aggregation is attributable to full wettability of the particles toward the minority fluid.

Supporting Information Figure S3 examines the same system as Figure 3 but at a particle loading of 40 wt %, and the trends of Figure 3 are repeated: with increasing water content, the system displays a network structure, growth of aggregates, complete separation, and finally phase inversion.

Supporting Information Figures S4 and S5 show systems with the same particle loading (20 wt %) as Figure 3 but with particles of different sizes. In Supporting Information Figure S4, the particle size ($\sim 35 \mu\text{m}$) is much larger and hence sedimentation is far more severe at all compositions. Most dramatically, at the highest water content after phase inversion has occurred, the oil drops are now sedimented, rather than floating in Figure 3. This is even though the oil density (0.83 g/mL) is lower than of water. This can be explained readily based on the surface-adsorption of the denser glass particles: calculations suggest that oil drops coated with $35 \mu\text{m}$ glass beads will have a net density exceeding that of water if the drop diameter is less than roughly 1.85 mm. Other than this difference in sedimentation behavior, the trends of Supporting Information Figure S4 parallel those of Figure 3.

In Supporting Information Figure S5, the particle size ($\sim 0.7 \mu\text{m}$) is much smaller than in Figure 3 ($\sim 5 \mu\text{m}$). This system is more complex than the previous two, because in the absence of water the particles do not disperse readily in oil and those that do disperse tend to form a particulate gel. Past research³⁰ on hydrophilic silica particles dispersed in low-polarity fluids suggests that such gel formation is driven by hydrogen-bonding attraction between the particles. Nevertheless, the broad trends remain the same, and in particular complete separation occurs below 10% water, followed by phase inversion. After phase inversion, the oil-in-water emulsion structure is not clearly evident on the vial-scale images in Supporting Information Figure S5, however the optical microscope image in Supporting

Information Figure S5 confirms that the aqueous phase in the 20% water sample contains oil drops.

Supporting Information Figure S6 tests an inverted system composed of highly hydrophobic particles. These particles were specified by the supplier to be modified by a trialkoxysilane in an aqueous process. These particles can adsorb at the oil/water interface, but confocal imaging suggests that most of the particles protrude strongly into the oil phase (Supporting Information Figure S2b). This system is inverted in the sense that the majority fluid is water (which is nonwetting toward these particles) whereas small quantities of wetting fluid oil are added. Unlike the previous examples, these experiments were conducted in vials that were not hydrophobically modified. Similar to the $0.7 \mu\text{m}$ particles, these particles are also aggregated to some extent. Furthermore, due to their high hydrophobicity in the absence of oil they do not disperse readily in water and hence tend to exhibit film climbing^{31,32} and coat the inner surface of the vial. In the absence of any added oil, some of the particles sink but remain aggregated. Addition of 2% or more of oil is sufficient to eliminate film climbing and induce large-scale aggregation in the bulk, followed by complete phase separation. The case of 7 and 10% oil in Supporting Information Figure S6 is especially interesting since the oil-rich phase (which is sunk due to the high density of the particles) takes on an irregular shape indicative of a yield-stress fluid. Between 10 and 30% of oil, the increasingly dilute oil-phase becomes both less dense and less viscous until at 30% oil it appears to have a completely smooth shape and floats at the surface. Finally, at 75% oil a phase-inverted structure is apparent, with water drops and particles both being sedimented to the bottom of the continuous phase oil. Optical imaging (Supporting Information Figure S6) shows that drops are on the order of $100 \mu\text{m}$ in diameter and are stabilized by particles adsorbed at the interface, albeit in the form of aggregates rather than a monolayer.

As a last example, Supporting Information Figure S7 shows an altogether different system where the two fluids are immiscible molten polymers, polyethylene oxide (PEO) and polyisobutylene (PIB), rather than oil and water. The particles used here are silica of $\sim 2 \mu\text{m}$ diameter, and they are almost completely wetted by PEO. Unlike oil and water, these polymeric fluids have a high viscosity (roughly 4 orders of magnitude higher than water at the 80° mixing temperature), and it is not possible to mix the fluids and the particles by simply shaking them together. Instead, they were mixed in a “Minimax” mixer³³ designed for melt-blending of polymers. Mixing was conducted at 80°C for 2 min using a rotor speed of 300 rpm. The particle loading was fixed at 20% and two PEO loadings were examined. Supporting Information Figure S7 shows that at 3 wt % PEO the sample has a pendular network with numerous capillary aggregates (Supporting Information Figure S7a). Upon raising the PEO loading to 7%, much larger aggregates appear, whereas the pendular network disappears almost completely (Supporting Information Figure S7b). The appearance of large aggregates is indicative of the strong tendency to undergo macroscopic phase separation. However, unlike in small molecule systems, these large aggregates do not sediment (and therefore do not coalesce into a separate layer) due to the high bulk viscosity and also because the blend is cooled after mixing causing the PEO to solidify. Supporting Information Figure S7c will be discussed later in the paper.

Finally a counter example was tested where particles were partially wetted by both phases rather than being almost fully

wetted by one phase. Online Supporting Information Figure S8 tests a system with partially hydrophobic particles. These were prepared by exposing the particles of Figure 3 to dimethylchlorosilane vapor in a rotary tumbler for 15 min. The fact that these particles are less hydrophobic than those of Supporting Information Figure S6 is evident from their better dispersibility in water (compare leftmost images in Supporting Information Figures S6 and S8) and from confocal imaging (compare Supporting Information Figure S2b and S2c). Ternary mixtures of these particles at 20 wt % loading with oil and water in various proportions shows behavior that sharply contrasts all the other systems in this paper: they do not show large aggregates, nor do they show macroscopic phase separation at any composition examined. Instead the mixtures have an opaque white appearance immediately after mixing. At longer times, sedimentation does occur, but the sediment is composed of drops of the minority fluid that do not coalesce, behavior typical of a stable Pickering emulsion. Optical microscopy (Supporting Information Figure S8) confirms that over most of the composition range, the structure consists of particle-covered drops (sometimes nonspherical) of the minority fluid.

On the basis of these results, we conclude that large aggregate formation and subsequent macroscopic phase separation is a general feature in ternary systems in which the particles are nearly completely wetted by one phase. Furthermore, in all the systems examined at 20 wt % particles, the amount and size of aggregates increases sharply at about 2–5% of the wetting fluid, and macroscopic phase separation occurs around 5–10% of the wetting fluid, i.e., aggregation and separation occur when the wetting fluid volume fraction is comparable to the particle volume fraction.

3.2. Morphological Map. We now turn to a more quantitative description of the compositions at which capillary networks, aggregates, macroscopically separated phases, or phase-inversion occur, or more specifically the boundaries marking compositions at which the morphology changes. These experiments were conducted only for the system of Figure 3 across a range of particle loadings ranging from 10 to 50 wt %. An immediate challenge in identifying transitions on the ternary composition diagram is that the structural changes occur continuously rather than abruptly. Even phase inversion, which can sometimes appear as a “catastrophic” event,^{34,35} does not appear at a sharply defined composition in such systems. Instead, with increasing amounts of water the aqueous phase encapsulates a successively larger fraction of oil drops until there is no free layer of oil at the surface. Accordingly, there is some arbitrariness in whether a system is to be classified as “macroscopically phase separated” or “phase inverted”. Thus some qualitative judgment is necessary for constructing a morphological map. The criteria of Table 2 proved adequate to achieve a consistent classification for our systems and were used in determining the symbols assigned to the various points in Figure 2. Because all the morphological transitions occur at relatively low water content, for clarity it is more convenient to replot the same data in rectilinear form (Figure 4). The chief trend that is qualitatively obvious is that the water content needed to induce all three transitions increases with increasing particle content.

Incidentally, the oil/water systems with the three other particle types from the Supporting Information can be classified in the same fashion and compared with Figure 4. We find that the morphologies realized with the hydrophilic particles (Supporting Information Figures S4 and S5) remain faithful

Table 2. Criteria for Classifying Morphologies

classification	description	color/symbol
pendular network	almost all of the aggregates are less than 2 mm	red square
aggregate	at least 3 aggregates are larger than 2 mm	blue circle
separated	1. aggregates coalesce to form a layer at the bottom of the vial 2. height of the layer of clear oil on top contains more than 50% of the total oil volume	yellow diamond
phase inverted	1. oil drops are encapsulated in the aqueous phase 2. height of the layer of clear oil on top contains less than 50% of the total oil volume	green square

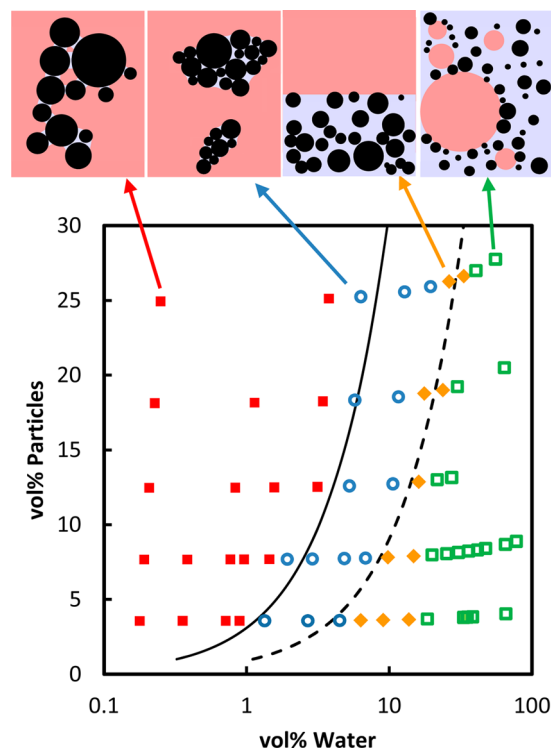


Figure 4. Morphological map for ternary system of Figure 3.

to the boundaries established in Figure 4. However, the composition for phase inversion does not appear to be universal; the amount of oil needed for phase inversion with the hydrophobic particles (Supporting Information Figure S6) is far larger than the amount of water needed for phase inversion with the hydrophilic ones.

It is worth reiterating that all the experiments of Figure 4 were conducted with hydrophobically modified vials. Section 2 had explained the reason; in samples with very small (<3%) of water, the aqueous phase tends to smear on the walls if the walls are hydrophilic. In effect, in these small sample sizes, the wettability of the walls influences aggregate formation. Analogously, the wettability of the walls may also affect the structure at high water content, for example, may affect the phase inversion composition. Our research has not tested this in particle-containing samples. Such wall effects are expected to diminish as sample size increases.

We close this Experimental Section with one incidental comment contrasting our observations with those made by

Koos et al.^{21,25,36} if the nonwetting fluid is in a minority, we invariably see Pickering emulsions and not a nonflowing gel state. A nonflowing gel-like state is seen in our systems only when the wetting fluid is in a small minority, inducing formation of a pendular network. This sharply contrasts the situations explored by Koos et al. where addition of a nonwetting fluid to particles suspended in a wetting fluid was found to induce gelation. The likely reason for this difference is that our particles are almost completely wettable by one of the fluids and can desorb off the interface, whereas those used by Koos had contact angles farther from 0 or 180° and remain adsorbed at the interface. Indeed later calculations by Koos²⁵ suggest that if the contact angle measured through the minority phase fluid exceeds roughly 160°, capillary clusters, which are the building blocks of a space-spanning network, are not stable.

4. DISCUSSION

The chief finding of this paper is that in ternary systems in which one fluid completely wets the particulate species, large aggregates appear when the wetting fluid is at a few percent loading, and macroscopic phase separation follows at slightly higher loading. In some ways, this finding is anticipated by previous research on the industrial process called “spherical agglomeration” in which a suspension of particles is forced to agglomerate by addition of a wetting fluid.^{37,38} The process is especially popular in the pharmaceutical industry and the word “spherical” is used because the process conditions are usually adjusted to realize spherical agglomerates. It is also used in the mineral or coal industry to recover small-sized coal particles.^{39–41} In that case, the coal particles are suspended in water and the wetting fluid is oil, and hence this process is also known as “oil agglomeration”.⁴¹ Most literature on spherical agglomeration is on complex real-world systems where surfactants are often used and the particles may be partially soluble in the wetting fluid. Moreover almost none of the articles in this area examine the microstructure or measure particle wettability. Nevertheless, the results consistently show that at wetting fluid/particle ratios ranging from 0.1–1, large and strong agglomerates form.^{39,41–43} At significantly lower wetting fluid/particle ratios, the aggregates are weak, whereas at significantly higher ratios, the aggregates are pasty,^{37,41,44} both of which are undesirable for agglomeration processes. An excellent example of the analogy between this older literature and the present work is the similarity between Figure 3 and a photograph of coal/oil/water suspensions published in a summary article in 1969.⁴³ For convenience, this photograph has been reproduced at the end of the Supporting Information. Although microscopic images were not provided in that paper, the discussion⁴³ suggests that the “flocs”, “pellets”, and “paste” in that paper correspond respectively a pendular network, large capillary aggregates, and macroscopic phase separation respectively.

Here, we will further discuss such aggregation and separation in our system. The discussion is framed for the specific case of hydrophilic particles so that water is the wetting phase and oil is the nonwetting fluid, but it applies more generally whenever one phase almost completely wets the particles. We propose that aggregate formation is bounded on one side by rheological considerations and on the other side by geometric considerations, and will discuss each of these in turn.

4.1. Rheology and Mechanics of Aggregates. Under conditions when $\phi_p \sim \phi_w$, if all the particles enter the water, the corresponding aqueous phase is a suspension with a high

effective volume fraction. For illustration, consider the sample from Figure 3 that has 20 wt % particles and 3 wt % water. If all the particles migrate into the water, the corresponding aqueous phase would have a particle volume fraction of 72.7%. Therefore, this suspension can have an extremely high viscosity and likely have a yield stress. Because phases with high viscosity or yield stress are difficult to breakup and emulsify, the formation of such a concentrated aqueous phase is an essentially irreversible process, i.e., once an aqueous blob of sufficiently high yield stress has formed, it cannot be broken easily, and hence large aggregates may be expected. Incidentally, the spherical agglomeration process mentioned above is a special case where a low level of agitation is maintained to “reshape” the aggregates into roughly spherical shapes by repeated collisions.

The aggregated state persists until the amount of water increases and dilutes the aggregates enough that they no longer have a significant yield stress. Beyond this water content, the aqueous phase behaves like “normal” fluid drops capable of breaking or coalescing. In our experiments, sedimentation of these relatively fluid drops leads to rapid coalescence and macroscopic phase separation. On the other hand, if sedimentation were prevented, for example, by continued mixing, the fluid drop size will likely be determined by the relative rate of breakup and coalescence processes. We emphasize that the above picture of aggregation and macroscopic separation is viable only if the particles are able to desorb into the wetting fluid, or equivalently, if the wetting fluid can engulf the particles completely. This picture becomes invalid if the particles remain irreversibly adsorbed at the interface, completely consistent with the lack of aggregation observed with the partially wettable particles of Supporting Information Figure S8.

Support for this physical picture comes from rheological measurements of particle-in-water suspensions for the 5 μm hydrophilic particles of Figure 3. Figure 5a shows the viscosity during stress ramp experiments for various particle weight fractions ranging from 68 to 75 wt %. Even though these measurements are conducted with stress ramps, the results show all the characteristics of concentrated suspension rheology measured under steady shear conditions:⁴⁵ a plateau in viscosity at low stress, a sharp decrease in viscosity over a narrow stress range, followed by gradual increase at high stress. The apparent yield stress, that is, the stress at which viscosity starts dropping sharply, can be obtained from these results and is plotted as a function of volume fraction in Figure 5b. The apparent yield stress increases sharply within this narrow composition range; at particle loadings below 68 wt %, it is no longer possible to measure the apparent yield stress reliably, whereas above 74 wt %, it is difficult to mix the sample homogeneously. If we arbitrarily choose an apparent yield stress of 1 Pa as being “sufficiently large”, the corresponding volume fraction is $\phi^* = 0.475$. We postulate that large aggregates will remain stable against coalescence if the particle volume fraction inside the aggregates exceeds this value, that is

$$\frac{\phi_p}{\phi_p + \phi_w} = \phi^* \quad (1)$$

This leads to

$$\phi_w = \left(\frac{1}{\phi^*} - 1 \right) \phi_p = 1.1\phi_p \quad (2)$$

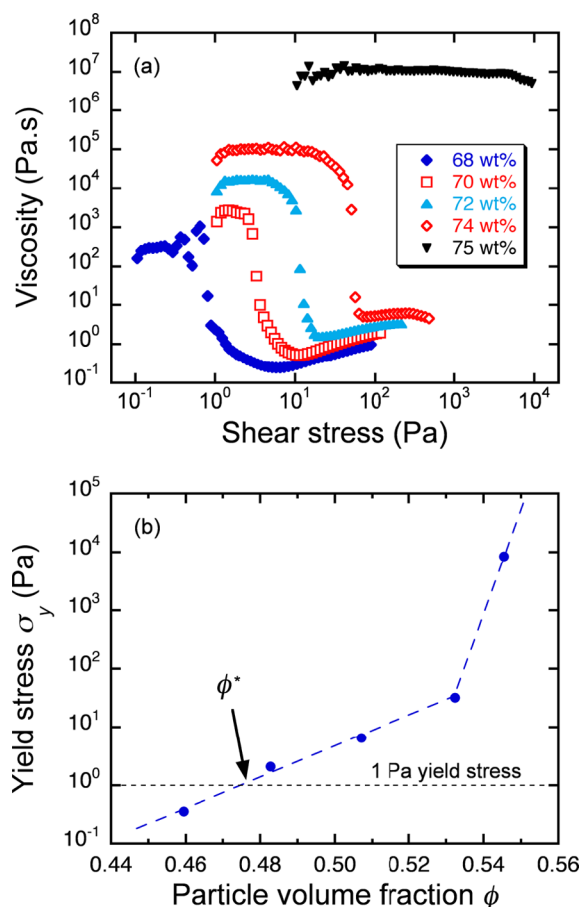


Figure 5. (a) Viscosity measured during stress ramp experiments on particle-in-water suspensions for the 5 μm hydrophilic particles at various particle loadings. (b) Estimated yield stresses.

where the last equality comes from substituting $\phi^* = 0.475$. Equation 2 represents the highest water concentration up to which aggregates remain solidlike, assuming that all particles migrate into the minority water phase. For water fractions higher than eq 2, the aggregates will be fluid-like (in effect drops of a concentrated suspension) and can coalesce readily and hence separate into layers. Equation 2 is shown as a dashed black line in Figure 4 and captures the transition from aggregate to macroscopic separation fairly well. Note any value ϕ^* between 0.44 and 0.54 gives comparably good agreement with the transition in Figure 4, thus some other criterion for determining ϕ^* , for example, divergence of viscosity, or an apparent yield stress of 10 Pa (rather than 1 Pa), would support the same physical picture.

This physical picture immediately suggests that aggregate formation will depend on the mixing protocol used, and in particular if the mixing process permits a large particle–water blob with a high yield stress to form, it will not break easily. To test this, a mixture with 20 wt % particles and 3 wt % water was prepared using three different mixing protocols. Figure 6a is the same image as the vial with 3% water in Figure 3; it corresponds to vortex-mixing the oil and water first, and then adding the particles. Figure 6b was prepared by placing the particles at the bottom of a vial, adding water, and then adding oil. Prior to adding oil, the contents of the vial correspond to an aqueous suspension with 72.7 vol% particles and presumably with a large yield stress. This mixing procedure therefore greatly increases aggregate formation. Indeed after vortex

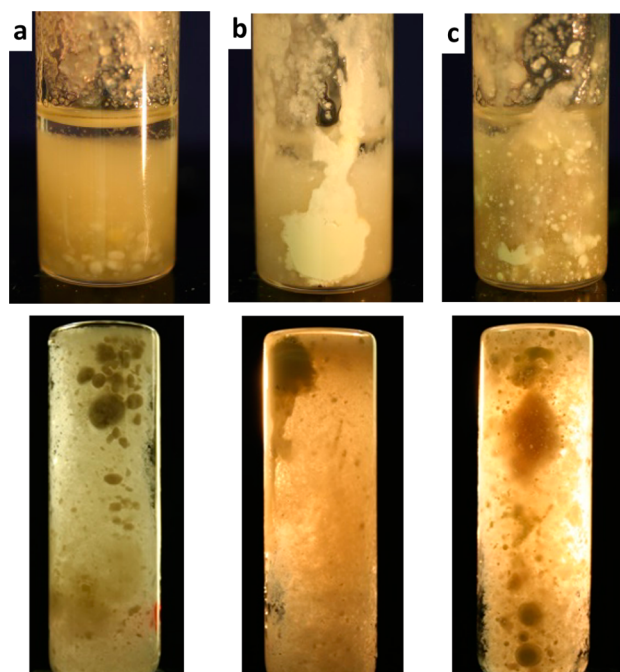


Figure 6. Effect of mixing protocol on the morphology of a sample with 20 wt % particles and 3 wt % water. See text for the mixing protocols used.

mixing a significant portion of the aqueous phase remains adhered to the bottom of the vial and has not dispersed at all. Figure 6c corresponds to the same procedure as Figure 6a, except that vortex mixing was conducted at the lowest vibration speed available; these mixing conditions permit far larger aggregates to persist as compared to Figure 6a.

These results suggest that an effective strategy to minimize aggregation may be to mix the two fluids as finely as possible, and then before significant coalescence, blend in the particles at high mixing intensity. This strategy is difficult to test with an oil/water system using our experimental methods and small sample sizes because the very low viscosity permits rapid drop settling and coalescence within seconds. However, this strategy was tested on the high viscosity system of Supporting Information Figure S7 where drop sedimentation and coalescence is slow. A sample was prepared with the same composition as Supporting Information Figure S7a but with a different mixing sequence: the minority phase PEO was first dispersed into the continuous phase PIB and then the particles were mixed in. The absence of large capillary aggregates in this mixture (Supporting Information Figure S7c) confirms that mixing the fluid phases prior to adding particles is indeed an effective strategy to avoid aggregation.

4.2. Geometry of Aggregation. Figure 6 suggests that with suitable mixing protocols or a higher mixing intensity, for example, using a high-pressure homogenizer, aggregate formation may be avoided altogether, and a truly pendular network may be obtained. Nevertheless, no matter how high the mixing intensity, we will argue that some level of aggregate formation is inevitable unless the volume fraction of water is extremely low. To understand why, consider the limiting case of a pendular network where all capillary interactions are strictly binary, that is, each meniscus binds exactly two particles together. Aggregate formation is initiated when a single meniscus can be shared by three or more particles, that is, when the meniscus is sufficiently large that the geometric

situation of Figure 7a is reached. Under these circumstances, aggregation will start either due to Brownian motion or due to any applied flow.

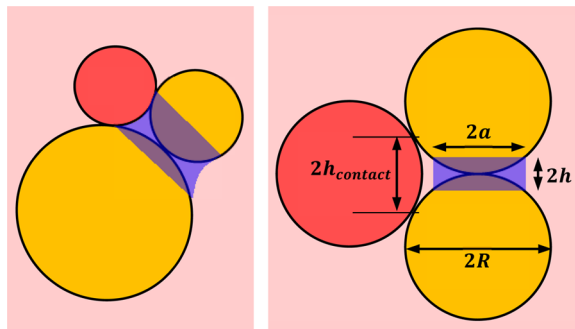


Figure 7. (a) A particle (red) joining an existing meniscus between two particles (yellow). (b) A simplified model assuming monodisperse particles and cylindrical meniscus.

To proceed further, we make three simplifying assumptions (Figure 7b) (1) the particles are monodisperse, (2) the menisci are also monodisperse, and (3) the menisci have cylindrical geometry. We may then write a mass balance that equates the net volume of the menisci to the total volume of the fluid added

$$z \frac{V_{\text{meniscus}}}{2} n_p = \phi_w \quad (3)$$

where V_{meniscus} is the volume of each meniscus, and z is the coordination number, that is, the number of menisci per particle. While the value of z is not known, for monodisperse particles it is bounded between 2 (corresponding to long chains of particles) and 12 (close packing). Given that a network of particles can form at a ϕ_p of only 9.5%, a relatively low value of z may be expected and below we will arbitrarily adopt a value of 4. The number of particles per unit volume n_p is given by

$$n_p = \frac{\phi_p}{\frac{4}{3}\pi R^3} \quad (4)$$

Furthermore, treating the meniscus as having cylindrical edges

$$\begin{aligned} V_{\text{meniscus}} &= 2 \left[\pi h^2 (2R - h) - \frac{\pi}{3} h^2 (3R - h) \right] \\ &= 2\pi h^2 \left[R - \frac{2}{3}h \right] \end{aligned} \quad (5)$$

Combining eqs 3–5, the meniscus dimensions h can be obtained. The resulting equation is cubic and must be solved numerically. However, assuming $h \ll R$ allows further simplification

$$V_{\text{meniscus}} = 2\pi h^2 R \quad (6)$$

Combining eqs 3, 4, and 6 gives

$$h = R \left(\frac{\phi_w}{z\phi_p} \frac{4}{3} \right)^{0.5} \quad (7)$$

The geometric criterion of Figure 7b corresponds to $h_{\text{contact}} = (1/2)(\sqrt{3} - 1)R = 0.27R$, and setting eq 7 to this value gives

$$\phi_w = z \frac{3}{16} (\sqrt{3} - 1)^4 \phi_p = 0.22\phi_p \quad (8)$$

where in the last equality, the value of z was arbitrarily set to 4. If the volume of water exceeds that given by eq 8, a purely pendular network would not be stable; under flow conditions, it is susceptible to aggregate formation. Equation 8 is plotted as the solid black line in Figure 4 and agrees reasonably well with the observed transition from a predominantly pendular network to a predominantly aggregated system.

We emphasize that the quantitative agreement of the results with eq 8 is somewhat fortuitous. First, as mentioned above, none of the morphological transitions in Figure 4 are sharp, and all are somewhat susceptible to qualitative judgment. Second, setting z to some value other than 4 would shift the solid black line. Finally, for polydisperse systems such as studied here the same geometric picture would predict aggregate formation at a lower volume fraction since small particles can more readily join the menisci between large particles. Thus the quantitative agreement is not as important as the basic idea that completely eliminating aggregates requires that the volume of the wetting fluid be far below the particle loading.

4.3. Analogy to Wet Granular Materials. This section seeks to place the observations here in the context of past literature on wet granular materials.^{46,47} The correspondence between our results and the spherical agglomeration process were already pointed out above. A similar, but more heavily studied process is “wet granulation”, widely used industrially for consolidation of powders.^{38,48} The process is similar to spherical agglomeration, except that the continuous phase fluid is air. Typically, a liquid binder is added to a powder being agitated in a tumbler or a fluidized bed to bind the particles into larger granules. As per the standard classification,⁴⁸ as the binder content is increased the following sequence of states appears: dry powder, pendular, funicular, capillary, and droplet. The first few of these states are completely analogous to the structures in Figure 3: the dry state (analogous to 0% water where capillary attractions are absent, the funicular state (at 0.2% water), and the capillary state (few percent water where large aggregates appear). A strictly pendular structure is not evident in Figure 3 but the results suggest that lower water contents below 0.2%, along with more intense mixing, would likely yield a pendular structure with minimal aggregation. Beyond a few percent water loading, the droplet state is expected, which corresponds to the “pasty” aggregates in the spherical agglomeration process. In our experiments, the droplet state is not seen because even though large drops may be present during vortex mixing, they sediment within seconds under quiescent conditions, leading to complete separation. The analogy with the granular systems breaks down at even higher water content because, phase inversion occurs in our systems, which has no analog in wet granular systems.

Incidentally, it is useful to compare, more quantitatively, the water contents at which the transitions appear. The geometrically derived factor of 0.22 in eq 8 agrees well with the rule of thumb that the transition from a pendular to funicular state appears when the liquid volume is about 25% of the particle volume.^{49,50} Interestingly, a factor of 0.14 is predicted⁵¹ from a different geometric argument based on the condition for merging two adjacent menisci of a pendular network. The factor of 1.1 in eq 2 is only somewhat larger than the empirical view that the capillary to the droplet state occurs when the liquid

volume is roughly equal to the particle volume.^{49,52} However eq 2 offers a more system-specific criterion because it is based on rheological measurements of the actual particle–water suspension. Specifically, the factor of 1.1 in eq 2 is directly related to the volume fraction of $\phi^* = 0.475$ at which this specific particle–water suspension develops a sufficiently high apparent yield stress. If different particles were to be used, ϕ^* would change, and so would the prefactor in eq 2. In particular, conditions that tend to increase the yield stress of the particle–water suspension, for example, interparticle attractions or large particle aspect ratio, will reduce ϕ^* , and hence allow aggregates to persist to a higher water content.

The observation that the ternary structure depends on the intensity and method of mixing (Figure 6) also parallels observations in the granulation literature. Specifically, a review article by Iveson⁵³ has cited several examples (especially Section 4.3.2.2 in that article) of granulation processes in which the granule size (analogous to aggregate size) decreased upon increasing mixing intensity. The effect of method of addition of the wetting fluid is less well-studied in the wet granular materials, however, one study has examined this issue in considerable detail. Knight et al.⁵⁴ examined granulation in a high shear mixer where the liquid was added in three different ways: poured all at once, sprayed during mixing, or added in solid form and melted during mixing. Not surprisingly, the pour-on method gave a far higher average size of granules, especially early during the mixing process. Similar to the results of Figure 6, once the liquid is poured onto the particle bed, large aggregates with a high particle content are formed, and subsequent breakup is unlikely.

Beyond these obvious analogies to structure of the ternary system, there are two further insights from the wet granular materials literature that may be relevant here.⁴⁷ The first is the role of interparticle friction. A capillary aggregate with a low water content has a negative curvature (as indicated by the concave meniscus of the fluid/fluid interface in the schematic of Figure 1d) and hence the internal pressure inside the granule is lower than the ambient pressure. Assuming that the typical negative radius of curvature is comparable to the particle size ($\sim 5 \mu\text{m}$), the corresponding capillary pressure α/R (where $\alpha \approx 0.05 \text{ N/m}$ is the interfacial tension) is about 10 kPa in our system. Unlike the familiar capillary pressure inside a spherical drop, this pressure is negative, that is, the interior of the aggregate has a lower pressure than the surroundings. Thus, the aggregates are under a significant hydrostatic pressure that forces the particles together and may induce significant frictional effects that can increase the yield stress. In the literature on wet granular materials, the Mohr-Coulomb model^{55,56} is often used to describe the dependence of the shear yield stress σ_y on the hydrostatic stress, p . For a simple loading situation of shearing a material under hydrostatic stress along the plane of shear, the Mohr-Coulomb model can be written as

$$\sigma_y = C + \mu p \quad (9)$$

In this equation, C is the cohesive stress between the grains due to their mutual attraction, and μ is the coefficient of friction. The apparent yield stress measured in the rheometer (when there is no hydrostatic stress) corresponds to the quantity C ; the second term is the additional yield stress due to the frictional contribution of the hydrostatic stress. The coefficient of friction is related to the angle of internal friction $\mu = \tan \varphi$, where φ can be taken equal to the angle of repose. For granular

materials, φ is roughly 30° corresponding to $\mu = 0.58$. In our case, we can estimate φ from tilting a vial containing a sedimented particles-in-water suspension until it flows. This yielded a comparable value of angle of repose. The exact value is not very important; the crucial point is that a value of μ between 0.1 and 1 may be expected, and hence the estimated hydrostatic pressure of 10 kPa would induce a shear yield stress on the order of a few kPa, comparable to the yield stress at the highest concentration examined in rheological studies in Figure 5. We conclude therefore that the rheological measurements, which are conducted on a bulk suspension of particles in water, may understate the yield stress of the capillary aggregates. In reality, the aggregates may be more difficult to break than judged from the shear rheological measurements. In effect, the interfacial tension may stabilize the capillary aggregates in two ways: the applied mixing stresses must not only overcome the interfacial tension, they must also overcome the additional friction caused by the negative capillary pressure inside the aggregates.

The second issue is the effect of particle size. Since capillary stresses scale inversely with particle size, the strength of wet granular materials, whether in the pendular, funicular, or capillary states, all increase as size reduces. Pierrat and Caram⁵⁷ have summarized the main equations governing the yield stress in all three states. The same idea applies to particle/liquid/liquid systems as well, and indeed Koos et al.³⁶ have shown that the yield stress of suspensions in a pendular state is proportional to reciprocal of the particle size. The implication of this size dependence of capillary forces is that the heavy aggregation phenomena discussed here will likely become even more important as particle size reduces.

5. CONCLUSIONS

This article adds to the growing knowledge of ternary particle/fluid/fluid systems that includes Pickering emulsions, bijels, wet granular media, and “dry liquids”. The chief conclusion of this paper is that ternary particle/liquid/liquid systems tend to aggregate heavily or completely separate into two layers if two conditions are met. The first is that the particles must be fully or almost fully wetted by one phase. Second, the wettable phase must be comparable in volume fraction to the particles. Under these conditions, particles can desorb into the wetting fluid and form a highly concentrated suspension phase that is difficult to disperse. Thus the apparent universality of aggregation and separation is rooted in the basic rheology of suspensions, viz. binary particle–fluid suspensions develop yield stresses (or become increasingly viscous) at high particle loadings. This also suggests that if the particles have high aspect ratio or attractive interactions that increase the tendency to form a yield stress fluid, large aggregates will appear over an even wider composition range. The effects of polydispersity are likely to be more complex: at a given particle/wetting fluid ratio, polydisperse particles will give aggregates of lower viscosity or yield stress,⁴⁵ thus allowing aggregates to coalesce or breakup more readily. On the other hand, polydisperse particles can pack more tightly and hence aggregates of higher particle loading (which are likely stronger) can be formed. Indeed in the spherical agglomeration literature, a certain proportion of “fines”, that is, small particles, are believed to improve agglomeration by making the agglomerates stronger.^{37,42} We also argue on geometric grounds that completely avoiding aggregation (i.e., obtaining a purely pendular network) requires the wetting fluid to be in an extremely small minority.

The most important practical implication is that if a ternary mixture is to be prepared under the two conditions listed at the beginning of this section, (1) homogeneous mixtures will be hard to prepare and (2) with high speed mixers or suitable mixing protocols, the tendency to aggregate may be mitigated. This is of particular relevance when ternary systems are used as a precursor for material synthesis.^{58–60} On the other hand, the same principles have been exploited in the spherical agglomeration process to separate particles suspended in a fluid by adding a second fluid that fully wets the particles. Finally, aggregation and separation appear only if the particles are fully wetted by one of the two fluids. Therefore an obvious practical strategy to discourage this type of aggregation is to add suitable surfactants that ensure partial wettability by both phases.

APPENDIX

Desorption of Particles by Viscous Forces during Mixing

The Introduction stated that “as the contact angle approaches either zero or 180°, the strength of the adsorption reduces sharply and particles can readily detach from interfaces, either due to thermal motion or due to external forces, for example, during mixing”. This point is explored further here.

A common way of illustrating the strength of adsorption is to compare the estimated desorption energy for a single particle, $\pi\alpha R^2(1 \pm \cos \theta)^2$ to the thermal energy kT for a situation such as Figure 8a. For particle diameters on the order of $R = 1 \mu\text{m}$,

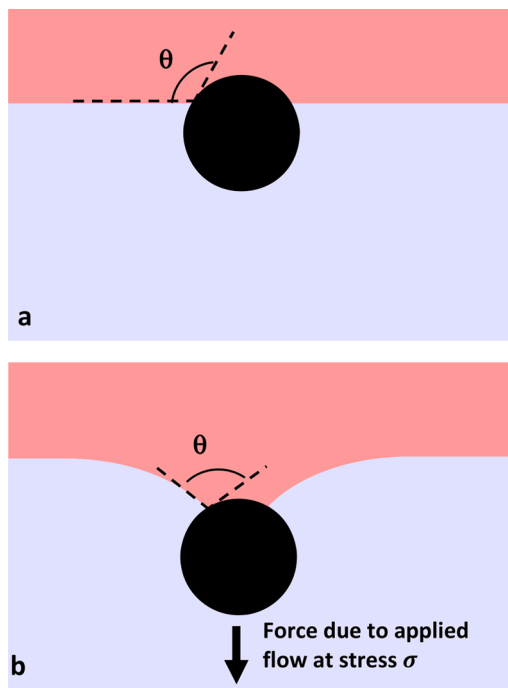


Figure 8. (a) A particle adsorbed at an interface under quiescent conditions. (b) An external force normal to the interface pulling the particle off the interface.

interfacial tension on the order of $\alpha = 0.05 \text{ mN/m}$, and a contact angle of 90° , the adsorption energy is 7 orders of magnitude higher than kT , thus guaranteeing that thermal fluctuations cannot detach the particles from the interface. However, a comparison against the thermal energy kT does not make any comment on the stability of particles at the interface

when external forces, for example, gravitational, magnetic, or due to mixing, are involved (Figure 8b). Most relevant to this paper are viscous forces during mixing and, as previously,²⁶ we consider a viscous force pulling a particle off an interface. Equating the force required to detach the particle from the interface, $2\pi\alpha R \cos^2(\theta/2)$, to the viscous force $\pi R^2\sigma$ where σ is the typical viscous stress experienced during mixing

$$2\pi\alpha R \cos^2\left(\frac{\theta}{2}\right) = \pi R^2\sigma$$

This yields an estimate for the stress required to detach the particle

$$\sigma = \frac{2\alpha}{R} \cos^2\left(\frac{\theta}{2}\right)$$

with the same values as above: $R = 1 \mu\text{m}$, $\alpha = 50 \text{ mN/m}$, and $\theta = 90^\circ$, the stress is estimated to be 50 kPa. But this stress drops as θ increases. For instance, at $\theta = 160^\circ$ the stress needed is only 3 kPa. If particle size were larger, the stress would be proportionately lower.

Finally, it is important to note that the energy required to detach particles from the interface scales with R^2 , whereas the corresponding viscous stress required to detach particles scales with R^{-1} . Thus as particle size increases, desorption due to thermal fluctuations becomes less likely, whereas desorption due to externally-applied viscous forces becomes more likely. In effect, a situation may be easily realized where particles with very large desorption energy may still not stay attached to the interface if even small external forces are present.

ASSOCIATED CONTENT

Supporting Information

Several figures discussed in the main text of the article as well as a reproduction of a photograph from Sirianni et al.⁴³ that was mentioned in Supporting Information Section 4. This material is available free of charge via the Internet at <http://pubs.acs.org>.

AUTHOR INFORMATION

Notes

The authors declare no competing financial interest.

ACKNOWLEDGMENTS

This work was supported by NSF-CBET Grants 0932901 and 1336311 and an undergraduate research supplement to the same grant. We are grateful to Ms. Patricia Begley, Prizmalite Corp., and Denka Corp. for providing the particles for this research. We thank Professor Rakesh Gupta, West Virginia University, for pointing us to the literature on spherical agglomeration, and Dr. Jason Devlin, Center for Biological Imaging at the University of Pittsburgh, for assistance with confocal imaging. The ternary diagram Figure 2 was drawn using a publicly available template prepared by David Graham and Nicholas Midgley.⁶¹

REFERENCES

- (1) Binks, B. P. Particles as surfactants - similarities and differences. *Curr. Opin. Colloid Interface Sci.* **2002**, *7* (1–2), 21–41.
- (2) Binks, B. P.; Horozov, T. S. *Colloidal particles at liquid interfaces*; Cambridge University Press: Cambridge, 2006.
- (3) Dickinson, E. Food emulsions and foams: Stabilization by particles. *Curr. Opin. Colloid Interface Sci.* **2010**, *15* (1–2), 40–49.
- (4) Horozov, T. S.; Binks, B. P. Particle-stabilized emulsions: A bilayer or a bridging monolayer? *Angew. Chem.* **2006**, *45* (5), 773–776.

- (5) Thareja, P.; Velankar, S. S. Particle-induced bridging in immiscible polymer blends. *Rheol. Acta* **2007**, *46* (3), 405–412.
- (6) Thareja, P.; Velankar, S. Rheology of immiscible blends with particle-induced drop clusters. *Rheol. Acta* **2008**, *47* (2), 189–200.
- (7) Lee, M. N.; Chan, H. K.; Mohraz, A. Characteristics of Pickering Emulsion Gels Formed by Droplet Bridging. *Langmuir* **2012**, *28* (6), 3085–3091.
- (8) Frost, D. S.; Schoepf, J. J.; Nofen, E. M.; Dai, L. L. Understanding droplet bridging in ionic liquid-based Pickering emulsions. *J. Colloid Interface Sci.* **2012**, *383*, 103–109.
- (9) Lee, M. N.; Mohraz, A. Bicontinuous Macroporous Materials from Bijel Templates. *Adv. Mater.* **2010**, *22* (43), 4836–4841.
- (10) Clegg, P. S. Fluid-bicontinuous gels stabilized by interfacial colloids: low and high molecular weight fluids. *J. Phys.: Condens. Matter* **2008**, *20* (11), 113101.
- (11) Tavecchi, J. W.; Thijssen, J. H. J.; Schofield, A. B.; Clegg, P. S. Novel, Robust, and Versatile Bijels of Nitromethane, Ethanediol, and Colloidal Silica: Capsules, Sub-Ten-Micrometer Domains, and Mechanical Properties. *Adv. Funct. Mater.* **2011**, *21* (11), 2020–2027.
- (12) Stratford, K.; Adhikari, R.; Pagonabarraga, I.; Desplat, J. C.; Cates, M. E. Colloidal jamming at interfaces: A route to fluid-bicontinuous gels. *Science* **2005**, *309* (5744), 2198–2201.
- (13) Fujii, S.; Iddon, P. D.; Ryan, A. J.; Armes, S. P. Aqueous particulate foams stabilized solely with polymer latex particles. *Langmuir* **2006**, *22* (18), 7512–7520.
- (14) Thareja, P.; Ising, B. P.; Kingston, S. J.; Velankar, S. Polymer foams stabilized by particles adsorbed at the air/polymer interface. *Macromol. Rapid Commun.* **2008**, *29* (15), 1329–1334.
- (15) Gonzenbach, U. T.; Studart, A. R.; Tervoort, E.; Gauckler, L. J. Stabilization of foams with inorganic colloidal particles. *Langmuir* **2006**, *22* (26), 10983–10988.
- (16) Murakami, R.; Bismarck, A. Particle-Stabilized Materials: Dry Oils and (Polymerized) Non-Aqueous Foams. *Adv. Funct. Mater.* **2010**, *20* (5), 732–737.
- (17) Binks, B. P.; Murakami, R. Phase inversion of particle-stabilized materials from foams to dry water. *Nat. Mater.* **2006**, *5* (11), 865–869.
- (18) Aussillous, P.; Quere, D. Liquid marbles. *Nature* **2001**, *411* (6840), 924–927.
- (19) Whitby, C. P.; Bian, X.; Sedev, R. Spontaneous liquid marble formation on packed porous beds. *Soft Matter* **2012**, *8* (44), 11336–11342.
- (20) Fujii, S.; Kameyama, S.; Armes, S. P.; Dupin, D.; Suzuki, M.; Nakamura, Y. pH-responsive liquid marbles stabilized with poly(2-vinylpyridine) particles. *Soft Matter* **2010**, *6* (3), 635–640.
- (21) Koos, E.; Willenbacher, N. Capillary Forces in Suspension Rheology. *Science* **2011**, *331* (6019), 897–900.
- (22) Vankao, S.; Nielsen, L. E.; Hill, C. T. Rheology of concentrated suspensions of spheres. 2. Suspensions agglomerated by an immiscible 2nd liquid. *J. Colloid Interface Sci.* **1975**, *53* (3), 367–373.
- (23) McCulfor, J.; Himes, P.; Anklam, M. R. The Effects of Capillary Forces on the Flow Properties of Glass Particle Suspensions in Mineral Oil. *AIChE J.* **2011**, *57* (9), 2334–2340.
- (24) Willet, C. D.; Johnson, S. A.; Adams, M. J.; Seville, J. P. K. Pendular capillary bridges. In *Handbook of Powder Technology*; Salman, A. D.; Hounslow, M.; Seville, J. P. K., Eds.; Elsevier: Amsterdam, 2007; Vol. 11, Chapter 28.
- (25) Koos, E.; Willenbacher, N. Particle configurations and gelation in capillary suspensions. *Soft Matter* **2012**, *8* (14), 3988–3994.
- (26) Nagarkar, S. P.; Velankar, S. S. Morphology and rheology of ternary fluid-fluid-solid systems. *Soft Matter* **2012**, *8* (32), 8464–8477.
- (27) Nagarkar, S.; Velankar, S. S. Rheology and morphology of model immiscible polymer blends with monodisperse spherical particles at the interface. *J. Rheol.* **2013**, *57* (3), 901–926.
- (28) Pawar, A. B.; Caggioni, M.; Hartel, R. W.; Spicer, P. T. Arrested coalescence of viscoelastic droplets with internal microstructure. *Faraday Discuss.* **2012**, *158*, 341–350.
- (29) Lopetsky, R. J. G.; Masliyah, J. H.; Xu, Z. Solid stabilized emulsions: A review. In *Colloidal Particles at Liquid Interfaces*; Binks, B. P., Horozov, T. S., Eds.; Cambridge University Press: Cambridge, 2006.
- (30) Raghavan, S. R.; Walls, H. J.; Khan, S. A. Rheology of silica dispersions in organic liquids: New evidence for solvation forces dictated by hydrogen bonding. *Langmuir* **2000**, *16* (21), 7920–7930.
- (31) Cheng, H. L.; Velankar, S. S. Film climbing of particle-laden interfaces. *Colloids Surf., A* **2008**, *315*, 275–284.
- (32) Binks, B. P.; Clint, J. H.; Fletcher, P. D. I.; Lees, T. J. G.; Taylor, P. Particle film growth driven by foam bubble coalescence. *Chem. Commun.* **2006**, *33*, 3531–3533.
- (33) Maric, M.; Macosko, C. W. Improving polymer blend dispersions in mini-mixers. *Polym. Eng. Sci.* **2001**, *41* (1), 118–130.
- (34) Binks, B. P.; Lumsdon, S. O. Catastrophic phase inversion of water-in-oil emulsions stabilized by hydrophobic silica. *Langmuir* **2000**, *16* (6), 2539–2547.
- (35) Pena, A.; Salager, J. L. Effect of stirring energy upon the dynamic inversion hysteresis of emulsions. *Colloids Surf. A* **2001**, *181* (1–3), 319–323.
- (36) Koos, E.; Johannsmeier, J.; Schwebler, L.; Willenbacher, N. Tuning suspension rheology using capillary forces. *Soft Matter* **2012**, *8* (24), 6620–6628.
- (37) Sparks, B. D.; Meadus, F. W. Spherical agglomeration in a conical drum. *Can. J. Chem. Eng.* **1977**, *55* (5), 502–505.
- (38) Pietsch, W. *Agglomeration Processes: Phenomena, Technologies, Equipment*; Wiley: Weinheim, 2008.
- (39) House, C. I.; Veal, C. J. Spherical agglomeration in minerals processing. In *Colloid and surface engineering: Applications in the process industries*; Williams, R. A., Ed.; Butterworth Heinemann: Oxford, 1992.
- (40) Capes, C. E.; Darcovich, K. A survey of oil agglomeration in wet fine coal processing. *Powder Technol.* **1984**, *40* (1–3), 43–52.
- (41) Chary, G. H. V. C.; Dastidar, M. G. Comprehensive study of process parameters affecting oil agglomeration using vegetable oils. *Fuel* **2013**, *106*, 285–292.
- (42) Chimmili, S.; Doraiswamy, D.; Gupta, R. K. Shear-induced agglomeration of particulate suspensions. *Ind. Eng. Chem. Res.* **1998**, *37* (6), 2073–2077.
- (43) Sirianni, A. F.; Capes, C. E.; Puddington, J. E. Recent experience with the spherical agglomeration process. *Can. J. Chem. Eng.* **1969**, *47* (2), 166–170.
- (44) Pietsch, W. Chapter 7: Tumble/growth agglomeration. In *Agglomeration Processes: Phenomena, Technologies, Equipment*; Wiley: Weinheim, 2008.
- (45) Larson, R. G. Particulate Suspensions. In *Structure and Rheology of Complex Fluids*; Oxford University Press: New York, 1999; Chapter 6.
- (46) Herminghaus, S. Dynamics of wet granular matter. *Adv. Phys.* **2005**, *54* (3), 221–261.
- (47) Strauch, S.; Herminghaus, S. Wet granular matter: a truly complex fluid. *Soft Matter* **2012**, *8* (32), 8271–8280.
- (48) Augsburger, L. L.; Vuppala, M. K. Theory of Granulation. In *Handbook of Pharmaceutical Granulation Technology*; Parikh, D. M., Ed.; Marcel-Dekker: New York, 1997; Chapter 2.
- (49) Capes, C. E. Agglomerate bonding. In *Particle Size Enlargement*; Elsevier: Amsterdam, 1980; Chapter 2.
- (50) Stanley-Wood, N. G. Size Enlargement. In *Principles of Powder Technology*; Rhodes, M. J., Ed.; Chichester: Wiley, 1990; Chapter 9.
- (51) Flemmer, C. L. On the regime boundaries of moisture in granular materials. *Powder Technol.* **1991**, *66* (2), 191–194.
- (52) Litster, J.; Ennis, B. J.; Liu, L. Particle and granule morphology. In *Science and Technology of Granulation Processes*; Kluwer Academic Publishers: Dordrecht, 2004; Chapter 2.
- (53) Iveson, S. M.; Litster, J. D.; Hapgood, K.; Ennis, B. J. Nucleation, growth and breakage phenomena in agitated wet granulation processes: a review. *Powder Technol.* **2001**, *117* (1–2), 3–39.
- (54) Knight, P. C.; Instone, T.; Pearson, J. M. K.; Hounslow, M. J. An investigation into the kinetics of liquid distribution and growth in high shear mixer agglomeration. *Powder Technol.* **1998**, *97* (3), 246–257.

(55) Massoudi, M. Constitutive modeling of flowing granular materials: A continuum approach. In *Granular Materials: Fundamentals and Applications*, Antony, S. J., Hoyle, W., Ding, Y., Eds.; RSC: Cambridge, 2004.

(56) Richefeu, V.; El Youssoufi, M. S.; Radjai, F. Shear strength properties of wet granular materials. *Phys. Rev. E* **2006**, *73* (5), 051304.

(57) Pierrat, P.; Caram, H. S. Tensile strength of wet granular materials. *Powder Technol.* **1997**, *91* (2), 83–93.

(58) Dittmann, J.; Koos, E.; Willenbacher, N. Ceramic Capillary Suspensions: Novel Processing Route for Macroporous Ceramic Materials. *J. Am. Ceram. Soc.* **2013**, *96* (2), 391–397.

(59) Brun, N.; Ungureanu, S.; Deleuze, H.; Backov, R. Hybrid foams, colloids and beyond: From design to applications. *Chem. Soc. Rev.* **2011**, *40* (2), 771–788.

(60) Menner, A.; Verdejo, R.; Shaffer, M.; Bismarck, A. Particle-stabilized surfactant-free medium internal phase emulsions as templates for porous nanocomposite materials: Poly-pickering-foams. *Langmuir* **2007**, *23* (5), 2398–2403.

(61) Graham, D. J.; Midgley, N. G. Graphical representation of particle shape using triangular diagrams: An Excel spreadsheet method. *Earth Surf. Processes Landforms* **2000**, *25* (13), 1473–1477.